Sci. Rep. RITU A44 (1997) pp. 181-185
No. 2, March 1997

SFM-IV Method for Characterizing Sub-Surface Interfaces of Semiconductor Devices

Masafumi Tanimoto

NTT Science and Core Technology Laboratory Group, 3-1 Morinosato Wakamiya, Atsugi-shi, Kanagawa 234-01, Japan

(Received January 22, 1997)

We demonstrate that a novel method of current-voltage (I-V) spectra measurement by scanning force microscopy (SFM) reveals subsurface local electrical characteristics of resonant tunneling diodes (RTDs) on a nanometer scale. Measured SFM I-V spectra of RTDs show negative differential resistance features, and the spatial resolution of this method was found to be 20 nm. Experimental evidence for the quantized nature of an SFM pointcontact was observed for the first time. High spatial resolution of this method was confirmed by a simple calculation for the area of current flow through RTD.

KEYWORDS: scanning force microscopy, resonant tunneling diode, negative difference resistance, quantized point contact, subsurface

1. Introduction

Characterization of electrical properties on a nanometer scale is important for fabricating deep- submicron Si devices and quantum-effect compound-semiconductor devices. Among the most important properties to be characterized are the electrical properties of subsurface interfaces. However, a conventional current-voltage (I-V) measurement yields properties averaged over several micrometers. Photoluminescence and cathodo-luminescence measurements, which are commonly used for characterizing heterostructures, are not electrical measurements and their spatial resolution is on a micrometer scale.

Scanning tunneling microscopy (STM) and scanning force microscopy (SFM) have been widely used to characterize semiconductor devices because of their high spatial resolution. To date these techniques have enabled two-dimensional delineation of p-n structures,[1-4] doping profiling[5,6] and potential distribution measurement.[7-9] However, these measurements only revealed local electrical properties on the topmost surfaces or cleaved surfaces of samples, and they gave no information about local current-voltage characteristics or local electrical properties of subsurface interfaces. One unique technique that makes it possible to observe the subsurface interface properties is ballistic electron emission microscopy (BEEM).[10] It reveals large spatial variation in Au/GaAs Schottky characteristics on a nanometer scale. However, most of the reported work has been limited to the characterization of Schottky barrier structures.

In this paper, we describe a novel method for characterizing resonant tunneling diodes (RTDs) by means of SFM I-V spectra. High spatial resolution of this method was confirmed by experimental evidence for the quantized nature of the SFM pointcontact and a simple calculation for the area of current flow through RTD.

2. Experimental

A schematic diagram of the setup for SFM I-V spectra measurement is shown in Fig. 1. The spectra were measured in the SFM contact mode. A ramp bias voltage with a typical sweeping time of 100 ms was applied between the lower electrode of the sample and the tip of the conductive cantilever. The current was monitored with a highly sensitive current-voltage amplifier connected to the cantilever. The SFM equipment used in this work is commercially available.[11] The minimum detectable currentis 10 pA and the maximum current is 100 nA. The measurements were carried out in an air ambient at room temperature. An Au/Cr-coated Si cantilever with a spring constant of 0.16 N/m was used for the measurement.

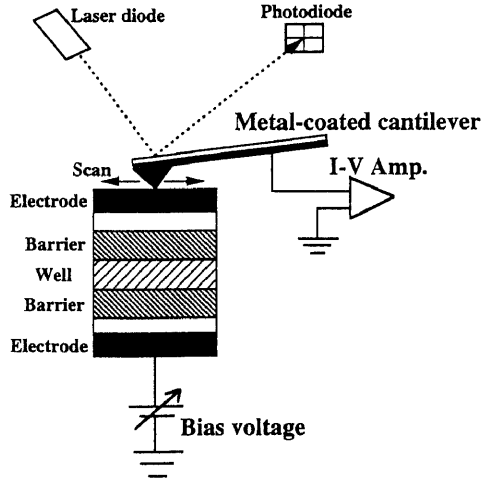

Fig. 1. Schematic diagram of setup for SFM I-V measurement. Bias voltage is applied between the lower electrode of the sample and the tip of the conductive SFM cantilever. The current is monitored by a current-voltage amplifier connected to the cantilever.

We used two different types of samples: a Schottky diode and an RTD. The Schottky diode was fabricated by evaporating a 20-nm-thick Au film on an n-type GaAs ($n=1\times10^{17}cm^{-3}$) substrate. RTDs having a GaAs (well)/ $Al_{0.3}Ga_{0.7}As$ (barrier) heterostructure were fabricated by metalorganic vapor phase epitaxy.[12] RTDs having a $In_{0.2}Ga_{0.8}As$ (well) / AlAs (barrier) heterostructure were fabricated by molecular beam epitaxy.[13] The well layer is

14 monolayers (ML) thick and the barrier layer is 12 ML thick for GaAs/AlGaAs RTDs. The well layer is 18 monolayers (ML) thick and the barrier layer is 11 ML thick for InGaAs/AlAs RTDs. Other structural parameters for GaAs/AlGaAs RTDs are metal electrode thickness of 300 nm, n^+-GaAs layer thickness of 350 nm, and undoped GaAs layer thickness of 30 nm, and those for InGaAs/AlAs RTDs are metal electrode thickness of 420 nm, n^+-GaAs layer thickness of 50 nm, and n-GaAs layer thickness of 270 nm. An n^+-GaAs layer were used to make ohmic contact with the heterosructure, and undoped GaAs layer or n-GaAs layer was used as a spacer layer between the n^+-GaAs layer and the barrier layer.

3. Results and Discussion

3.1 SFM I-V spectra

To study the feasibility of the SFM I-V spectra method, we first used the Au/GaAs Schottky diode, since its local electrical properties were studied in detail by Kaiser and Bell[10] using BEEM. Typical SFM I-V spectra for the Au/GaAs Schottky diode were measured by a conventional prober and our SFM methods. The rectifying spectra were obtained by both methods, and they are shown in Fig.2.

The spatial resolution of this SFM I-V method was determined experimentally as follows. The Schottky diode was degraded locally by injecting excess current through a diode, and we obtained a linear I-V characteristic which is depicted as a dotted line in Fig. 2(b). The site where the spectrum shows a linear feature is designated as a breakdown site. In contrast, the site showing a rectifying feature is designated as a normal site. We define the spatial resolution to be the minimum distance between the breakdown site and the normal site. We found the spatial resolution to be less than 5 nm for a Schottky diode with 20-nm-thick Au. Detailed analysis of spatial resolution will be described in a later section.

Figure 3 shows typical I-V spectra of an RTD measured by a conventional prober and our SFM methods. The SFM spectrum (Fig. 3(b)) shows negative differential resistance (NDR) features at bias voltages of 0.95 and -0.6 V, similar to those obtained by a conventional prober method. We observed the peak-to-valley current ratio of 1.8

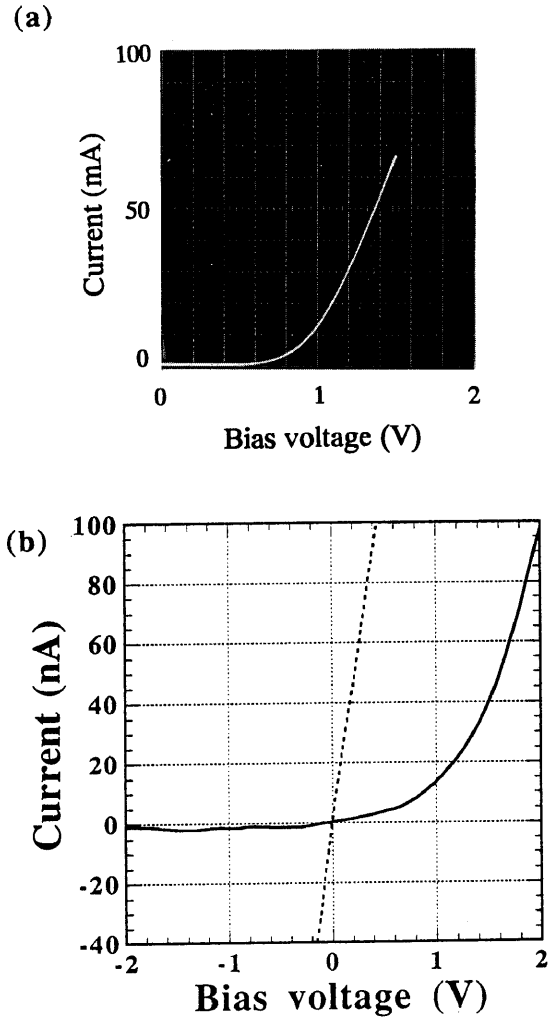

Fig. 2. I-V spectra for a Au/GaAs Schottky diode measured by (a) conventional prober method and (b) SFM I-V method. The solid line in (b) shows normal rectifying I-V characteristics. The dotted line in (b) shows a degraded I-V characteristic obtained by injecting an excess current through the diode.

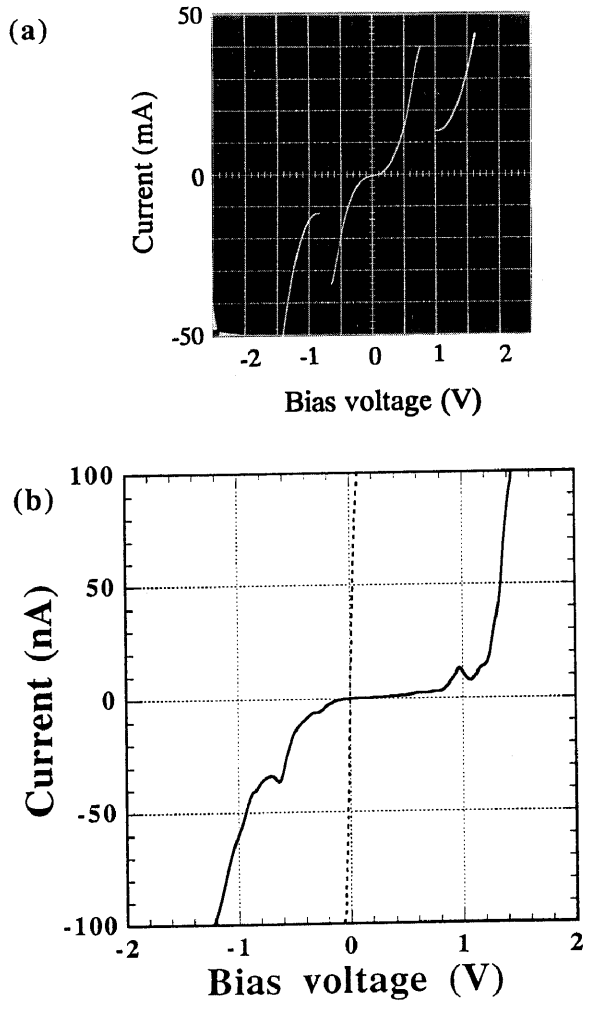

Fig. 3. I-V spectra for a GaAs/AlGaAs RTD measured by (a) conventional prober method and (b) SFM I-V method. The solid line in (b) shows negative differential resistance features. The dotted line in (b) shows a degraded I-V characteristic obtained by injecting an excess current through the diode.

with a small peak voltage shift in the positive bias region. The observed small peak current in the SFM spectrum is less than one-millionth of that observed by a conventional prober method. This indicates that the current flows in a small area of a few hundred square nanometers. The peak voltage shift is attributable to the potential drop in the n^+-GaAs layer, which will be described in a later section. The spatial resolution was experimentally determined to be 20 nm for the RTD used in this work.

The SFM I-V spectra reflect the subsurface electrical properties when the tip is located within a grain boundary of the electrode metal. Hence, a two-dimensional current image at a constant bias voltage obtained by scanning the tip over the top electrode can reveal spatial variations in subsurface electrical characteristics. Figure 4 shows a topographic image and a two-dimensional current image for InGaAs RTD 200 nm x 200 nm in area at a constant bias voltage of 0.8V. The current image shows bright regions corresponding to a large current of more than 100 nA, intermediate brightness regions corresponding to a current of 20 nA, and dark regions corresponding to a small current of less than 1 nA. The intermediate regions are observed between the bright an the dark regions. Since we found no relationship between the surface morphology and the current image, the current distribution is considered to reflect device structural fluctuation at subsurface interfaces. Detailed analysis[13] for this result reveled that the large current difference between bright and dark regions reflects one-monolayer fluctuation in well thickness and small current difference between intermediate and dark regions reflects deviation in the In mole fraction for an InGaAs well.

3.2 Analysis of high spatial resolution

The high spatial resolution of this method is explained by the collimated carrier injection[14] from the quantized pointcontact[15] to the metal electrode, the potential drop in the n^+-GaAs region, and the nonlinear I-V characteristics of the heterostructure.

3.2.1 Quantized point-contact nature and collimated carrier injection

Evidence for the quantized nature of an SFM pointcontact was obtained through contact resistance measurement with varying force imposed on an SFM tip. An SFM tip covered with thin metal film shows a high contact resistance of more than $1x10^7\ \Omega$, and its contact resistance can easily become infinite during the measurement. However, by employing a 40-nm-thick Au/10-nm-thick Cr double metal layer, contact resistance of an SFM tip was reduced to about $1x10^4\ \Omega$. This SFM tip showed quantized pointcontact nature. Figure 5 shows the dependence of the contact resistance between an SFM tip and sample (graphite) on the imposed force. For these measurements, we used graphite as a sample because it has an atomically flat surface and uniform electrical characteristics. The contact resistance is quantized in units of $h/2e^2$ as indicated by the abrupt drop in the low force region. In contrast, if contact resistance exhibits macroscopic characteristics, the contact resistance should be proportional to the minus two-thirds power of the force imposed on an SFM tip and show continuous values.

In addition to the point-contact nature, a blunt SFM tip apex can collimate the carrier beam injected from the SFM tip into the metal electrode to some extent. The collimation is caused by the flaring of the potential boundary of the SFM tip[14] and the full opening angle of the carrier beam[14] is mostly determined by the shape of the tip. The full opening angle was calculated to be as small as 6°. Moreover, the electric field perpendicular to the electrode in the metal region may suppress lateral carrier diffusion. As a result, current is injected into a small area at the electrode/n^+-GaAs interface. We estimated the injected current radius r_i at this interface to be about 10 nm.

3.2.2 Fine structure in I-V spectra

On closely inspecting SFM I-V spectra for RTD, shown in Fig. 3(b), we found fine structure in the I-V

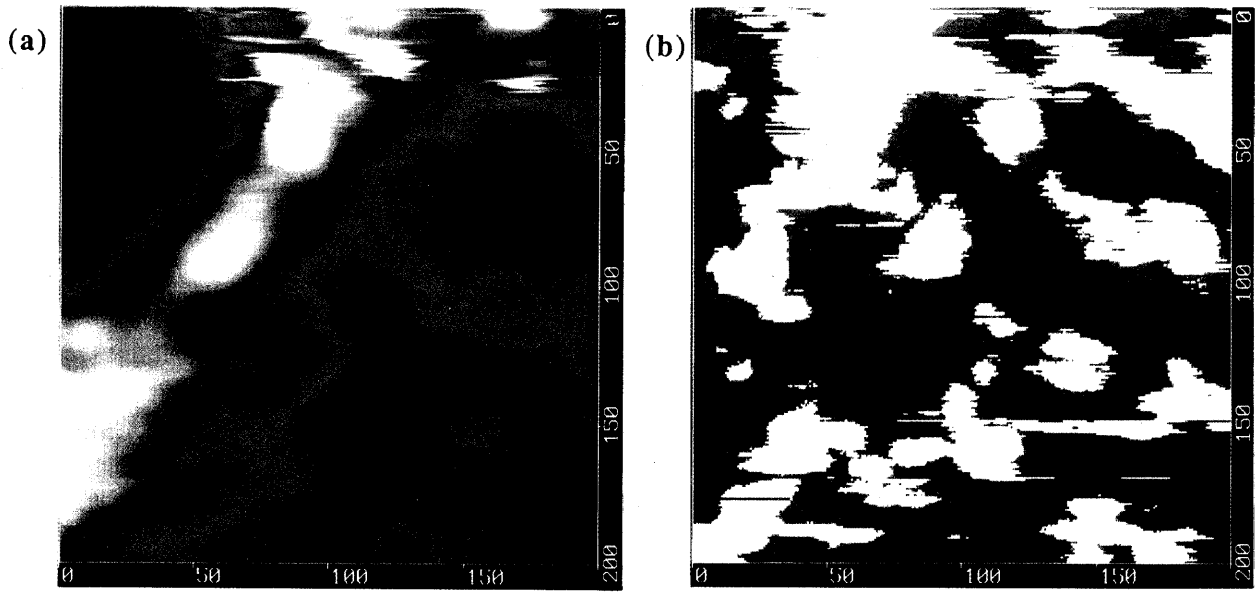

Fig. 4. (a) Topographic image for the surface of metal electrode and (b) two-dimensional current image for InGaAs RTD. Scanning area is 200 nm x 200 nm. The measured current is less than 1 nA for a dark region, 20 nA for an intermediate region and more than 100 nA for a bright region.

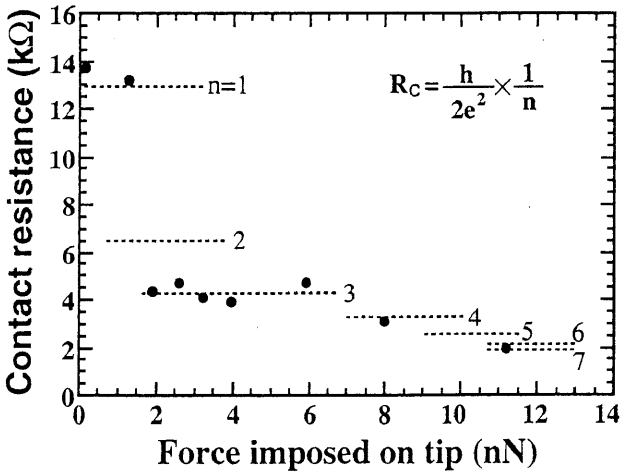

Fig. 5. Dependence of contact resistance between SFM tip and sample (graphite) on imposed force. Observed contact resistance is quantized in units of $h/2e^2$. Dotted lines parallel to the horizontal axis correspond to the calculated resistance values of $h/2ne^2$ (n:integer).

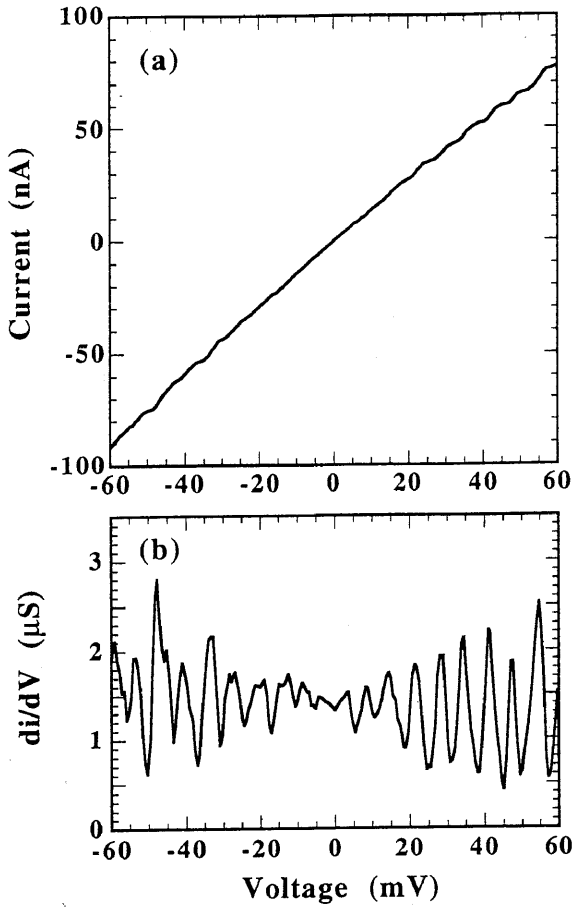

Fig. 6. (a) SFM I-V spectrum obtained for graphite. The spectrum shows steplike characteristics. (b) Current derivative showing clear peaks about 6 mV apart.

spectrum at voltages below and above the peak voltage. The derivative of the spectrum shows conductance oscillation with a period of about 100 mV. The same is true for the Schottky diode, as shown in Fig. 2(b). To study the fine structure we used graphite as a sample. Figure 6(a) shows the SFM I-V spectrum for graphite, which shows a relatively high contact resistance of 750 kΩ. The spectrum shows current oscillation, or steplike characteristics. The derivative of the spectrum, shown in Fig. 6(b), shows clear periodic peaks about 6 mV apart. These features are reproducible. They did not depend on the measurement conditions; sweeping time of ramp bias voltage, number of sampling, or holding time before I-V spectra measurement. Moreover, it is interesting to note that the difference in amplitude of adjacent peaks shows discrete values rather than continuous values, as shown in Fig. 7. The unit value was found to be 0.47 μS. This result implies that the observed I-V spectrum reflects some quantized carrier transport.

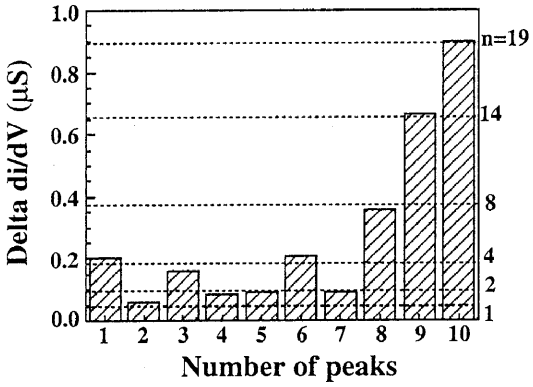

Fig. 7. Difference in the amplitude of adjacent peaks of the current derivative shown in Fig. 6(b). Dotted lines parallel to the horizontal axis correspond to the calculated values of n x 0.47μS (n:integer).

One of the possible mechanisms explaining the conductance oscillation may be the carrier lateral confinement under the tip. Considering the large difference in the oscillation periods for RTD and graphite by a factor of ten, we can conclude that the conduction oscillation originates from the carrier lateral confinement in the tip/sample interface region for graphite and in the metal/n^+-GaAs interface region for RTDs. The fine structure in the I-V spectra has already been observed for submicron-diameter RTDs[16-18] and it was considered to originate from the carrier transport in the heterostructure of RTDs. In contrast to these reports, our results imply that the carrier lateral confinement induced by the pointcontact plays an important role. All the spectra, however, were measured with a limited force condition (a small tip force of 0.16 nN: standard force condition for SFM measurement), and therefore we need more detailed experiments and analyses to investigate the conductance oscillation more thoroughly.

3.2.3 Radius of current flow in heterostructure

The current injection in a small area at the electrode/n^+-GaAs interface allows us to assume a conical current flow through the n^+-GaAs and the heterostructure for calculating an effective current radius r_e in the heterostructure. For the calculation, we took account of the nonlinear I-V characteristics of RTD. Nonlinearity was estimated from the spectrum shown in Fig.2(a); when the bias voltage applied to the sample decreases from the peak

voltage V_p to one-half of that, the current decreases by 80 %. Figure 8 shows the calculated result for the dependence of the effective current radius r_e in the heterostructure on the injected current radius r_i at the electrode/n+-GaAs interface. r_e increases with r_i and has a small value of about five times larger than r_i even though carriers travel a long distance through the n+-GaAs and the heterostructure.

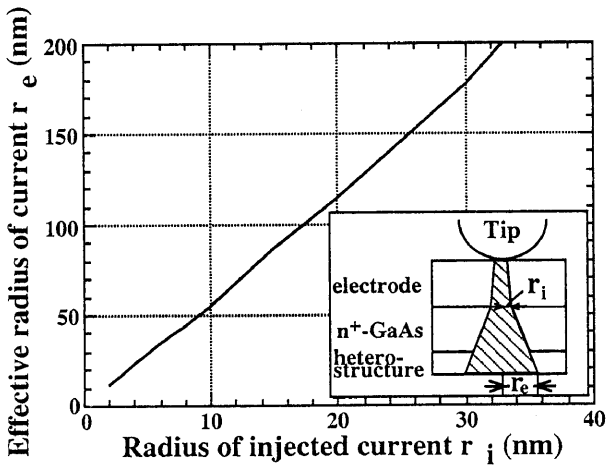

Fig. 8. Dependence of the effective currentradius re in the heterostructure on injected currentradius ri at the electrode/n+-GaAs interface. The inset shows a schematic drawing of the current flow.

This current concentration in a small area can be ascribed to the potential drop in the n+-GaAs region and the nonlinear I-V characteristics of the RTD. A potential drop is caused by the difference in the current-radius r dependence of the resistance for the n+-GaAs and for the heterostructure. For the n+-GaAs layer, resistance is proportional to r^{-1}, while for the heterostructure, it is proportional to r^{-2}. Thus, the potential drop in the n+-GaAs layer increases with the radii of the currents. This causes a reduction in the voltage across the heterostructure, and an abrupt decrease in the current according to the nonlinear I-V characteristics of RTD. When injected current radius r_i is 10 nm, effective current radius r_e in the heterostructure is calculated to be 55 nm, which is in agreement with the measured spatial resolution of 20 nm.

4. Conclusions

A novel nanometer-scale electrical characterization method using SFM I-V spectra was proposed and successfully applied to evaluating subsurface interface characteristics of RTDs. The measured spatial resolution of this method was found to be as small as 20 nm for this RTD. The quantized nature of SFM tip pointcontact was observed for the first time. The high spatial resolution can be explained on the basis of simple calculations. The current concentration is ascribed to the collimated carrier injection from the quantized pointcontact to the metal electrode, the potential drop in the n+-GaAs region, and the nonlinear feature of RTD spectra. The fine structure showing the steplike characteristics in SFM I-V spectra was also observed for RTD, Schottky diode, and graphite.

Acknowledgments

The author would like to thank K. Kanisawa and M. Shinohara for providing the samples and useful discussions. He also thank H. Taniyama, H. Fukuyama, and M. Yamamoto for their helpful comments. He is also grateful to N. Inoue, A. Yoshii, and Y. Imamura for their encouragement throughout this work.

1) S. Hosaka, S. Hosoki, K. Tanaka, K. Horiuchi and N. Natsuaki: Appl. Phys. Lett. **53** (1988) 487.
2) C. Shafai and D.J. Thomson and M. Simard-Normandin: J. Vac. Sci. Technol. B **12** (1994) 378.
3) K.Yamazaki and S.Nakajima: Jpn. J. Appl. Phys. **33** (1994) 3743.
4) M. Nonnenmacher, M. O'Boyle and H.K. Wickramasinghe: Ultramicroscopy: **42-44** (1992) 268.
5) C. C. Williams, J. Slinkman and H. K. Wickramashinghe: Appl. Phys. Lett. **55** (1989) 1662.
6) T. Takigami and M. Tanimoto: Appl. Phys. Lett. **58**(1991) 2288.
7) P. Muralt, H. Meier, D.W. Pohl and H.W. Salemink: Appl. Phys. Lett. **50** (1987) 1352.
8) M. Tanimoto and K. Arai: J. Vac. Sci. Technol. B **12** (1994) 2125.
9) O. Vatel and M. Tanimoto: J. Appl. Phys **77** (1995) 2358.
10) W.J. Kaiser and D.J. Bell: Phys. Rev. Lett. **61** (1988) 1406.
11) Seiko Instruments: SPI3700/SPA300.
12) M. Shinohara, M. Tanimoto, H. Yokoyama and N. Inoue: Appl. Phys. Lett. **63** (1994) 1256.
13) K. Kanisawa and M. Tanimoto: Jpn. J. Appl. Phys. **34** (1995) 4466.
14) L.W. Molenkamp, A.A.M. Staring, C.W.J. Beenakker, R. Eppenga, C.E. Timmering, J.G. Williamson, C.J.P.M. Harmans and C.T. Foxon: Phys. Rev. Lett. **41** (1990) 1274.
15) L. Olesen, E. Lægsgaard, I. Stengaard, F. Besenbacher, J. Schiøtz, P. Stoltze, K.W. Jacobsen and J.K. Nørskov: Phys. Rev. Lett. **72** (1994) 2251.
16) M.A. Reed, J.N. Randall, R.J. Aggarwal, R.J. Matyi, T.M. Moore and A.E. Wetssel: Phys. Rev. Lett. **60** (1988) 535.
17) A.Groshev: Phys. Rev. B, **42** (1990) 5895.
18) J.-W. Sakai, T.M. Formhold, P.H. Beton, L. Eaves, M. Henini, P.C. Main, F.W. Sheard and G. Hill: Phys. Rev. B, **48** (1993) 5664.